Amino Acids (2014) 46:2015–2024
DOI 10.1007/s00726-014-1750-y

ORIGINAL ARTICLE

# Design of p53-derived peptides with cytotoxicity on breast cancer

**Yi Fang · Rongzhong Jin · Yinqi Gao · Jidong Gao · Jing Wang**

Received: 12 March 2014 / Accepted: 14 April 2014 / Published online: 15 May 2014


**Abstract** The tumor suppressor p53 plays essential role in conserving stability by preventing genome mutation, which is inactivated naturally by its negative regulator MDM2. Thus, targeting p53–MDM2 protein–protein interaction has been raised as a new cancer therapy in the medicinal community. In the current study, we report a successful application of an integrative protocol to design novel p53-derived peptides with cytotoxicity on human breast cancer cells. A quantitative structure–activity relationship-improved statistical potential was used to evaluate the binding potency of totally 24,054 single- and dual-point mutants of p53 peptide to MDM2 in a high-throughput manner, from which 46 peptide mutants with high predicted affinity and typical helical feature were involved in a rigorous modeling procedure that employed molecular dynamics simulations and post-binding energy analysis to systematically investigate the structural, energetic and dynamic aspects of peptide interactions with MDM2. Subsequently, a biological analysis was performed on a number of promising peptide candidates to determine their cytotoxic effects on human breast cancer cell line MDF-7. Six dual-point mutants were found to have moderate or high activities with their $IC_{50}$ values ranging from 16.3 to 137.0 μM, which are better than that of wild-type p53 peptide ($IC_{50}$ = 182.6 μM) and close to that of classical anticancer agent *cis*-platin ($IC_{50}$ = 4.3 μM). Further, the most active peptide ETFSDWWKLLAE was selected as parent to further derive new mutants on the basis of the structural and energetic profile of its complex with MDM2. Consequently, three triple-point mutants (LTFSDWWKLLAE, ESFSDWWKLLAE and ETFADWWKLLAE) were obtained, and their biological activities ($IC_{50}$ = 15.1, 27.0 and 8.7 μM, respectively) were determined to be comparable or better than the parent ($IC_{50}$ = 16.3 μM).

**Keywords** p53 protein · MDM2 · Peptide · Cytotoxicity · Breast cancer

Y. Fang · Y. Gao · J. Gao (✉) · J. Wang (✉)
Department of Breast Surgical Oncology, Cancer Hospital, Chinese Academy of Medical Sciences and Peking Union Medical College, Beijing 100021, China
e-mail: ab168@cicams.ac.cn

J. Wang
e-mail: jjing_wang@126.com

R. Jin
College of Biotechnology, Guilin Medical University, Guilin 541004, China

## Introduction

Breast cancer is the most common cause of cancer among women in both high-resource and low-resource settings, which is responsible for over one million of the estimated 10 million neoplasms diagnosed worldwide each year (Bray et al. 2004), accounting for 23 % of the total cancer cases and 14 % of the cancer deaths (Jemal et al. 2011). Although some highly successful treatments have been developed, most breast tumors are resistant to conventional therapies and a considerable number of them relapse (Caffarel et al. 2012). Therefore, new strategies are urgently needed, and the challenge for the future will most likely be the development of chemotherapeutic agents with low toxicity and side-effect that can specifically target patient's tumors.

The tumor suppressor p53 protein has been found to play an essential role in the development and progressing of breast cancer and many other tumors. p53 functions to eliminate and inhibit the proliferation of abnormal cells,

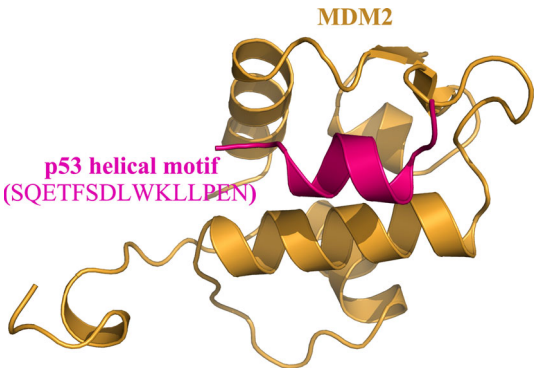


**Fig. 1** The crystal structure of p53 helical motif in complex with MDM2 (PDB: 4HFZ), where a typical peptide-mediated interaction can be observed

thereby preventing neoplastic development. Mutation of the p53 gene is a common occurrence in breast cancer but is by no means universal (Coles et al. 1992). Changes, both genetic and epigenetic, have been identified in regulators of p53 activity and in some downstream transcriptional targets of p53 in breast cancer that express wild-type p53 (Gasco et al. 2002). Very recently, the p53 has also shown predicting role in primary diagnosis to death for visceral metastasis breast cancer patients (Yang et al. 2013).

In tumors where p53 is not mutated, its function is inhibited by overexpression of its negative regulator MDM2, which binds to the N-terminal transactivation domain of p53. The p53–MDM2 system forms an autoregulatory feedback loop; as a transcription factor p53 interacts with the promoter and increases expression of the MDM2 gene. In turn, MDM2 protein directly binds to p53 and downregulates the activity of p53 through multiple mechanisms (Wang et al. 2012). Interference of the p53–MDM2 interaction should therefore lead to both the nuclear accumulation and the activation of p53 followed by the death of tumor cells from apoptosis, and the p53–MDM2 inhibitors might be attractive new anticancer agents that could be used to activate wild-type p53 in solid tumors (Chene 2004).

The p53 binds to MDM2 through a helical motif in its N-terminal domain (Chi et al. 2005), forming a typical peptide-mediated interaction (Petsalaki and Russell 2008) at the p53–MDM2 interface (Fig. 1). Previously, massive efforts have been addressed on discovery of MDM2 binding peptides to abolish this interaction. Such experimental techniques as phage display and peptide library have been developed to successfully determine the peptide ligands recognized by MDM2 (Hu et al. 2007). The accuracy of peptide ligands is still limited by the coverage of the entire structural space so that most obtained peptides only show weak affinity and low specificity for MDM2, which thus cannot be used as good competitors to disrupt the cognate p53–MDM2 interaction. Later, structure-based design of peptide antagonists inhibiting the interaction was proposed based on the high resolution crystal structure of p53–MDM2 complex architecture (Anil et al. 2013) and, recently, a systematic Ala scanning mutational analysis and binding assay of peptide interaction with MDM2 was reported to elucidate the molecular determinants for peptide activity and specificity (Li et al. 2010). However, it is too time-consuming and expensive to perform crystallographic analysis of even a quite limited quantity of MDM2–peptide systems and, from which, use the binding assay to identify potent MDM2 binders. Therefore, only very few peptides and peptidomimetics have been published to date that possess affinities towards the p53 binding site of MDM2 in the nanomolar range (Popowicz et al. 2011).

In the current study, we attempted to systematically examine the binding behavior of all single-point and dual-point mutants of the p53 helical motif to MDM2 and, on this basis, to design p53-derived peptides with cytotoxicity on human breast cancer cells. To achieve this, we proposed a synthetic bioinformatics protocol that integrated statistical potential screening, quantitative structure–activity relationship (QSAR) modeling, atomistic molecular dynamics (MD) simulations and post molecular mechanics/generalized Born surface area (MM/GBSA) calculations (Zhou et al. 2013) to investigate the binding phenomenon of various peptide ligands to MDM2 receptor at molecular level. We successfully employed this protocol to design an array of p53 peptide mutants that have potential capability to target MDM2 with high affinity, from which several highly promising candidates were assayed for their cytotoxicity on breast cancer cell line MCF-7 to validate results arising from the theoretical modeling. We also gave a detailed discussion of structural basis, energetic property and biological implication underlying the intermolecular interaction between the MDM2 and its peptide ligands.

## Materials and methods

### QSAR-improved PPRCP

Recently, Han et al. (2013) have developed a quantitative structure–activity relationship-improved protein–peptide residue contact potential (QSAR-improved PPRCP) to perform high-throughput inference of protein–peptide binding affinities at structure level. This method was employed here to evaluate the relative binding strength of various p53 peptide mutants to MDM2 protein. A brief description of generating the QSAR-improved PPRCP is summarized as follows:

1. A total of 505 unique protein–peptide interface clusters were collected from the PepX database (Vanhee et al. 2010). These clusters cover 1,431 PDB-deposited structures containing complexes with peptides bound to MHC, thrombins, SH3 domains, PDZ domains, α-ligand-binding domains and others, which have high crystallographic resolution and appropriate amino acid composition.
2. The interface of a complex cluster was defined as the assembly of all contact residues between protein and peptide; two residues separately coming from protein and peptide were considered in contact if there was a hydrogen bond, a van der Waals interaction, or at least one pair of non-hydrogen atoms separated by a distance <6 Å between them (Zhou et al. 2010).
3. A knowledge-based statistical potential, namely PPRCP, was derived from the defined interfaces of the 505 complex clusters on the basis of classical potential of mean force (PMF) theory (Mitchell et al. 1999), which describes interaction preference for each of the 20 × 20 types of residue contact at protein–peptide interface.
4. The unsupervised statistical potential PPRCP was calibrated with a supervised QSAR approach based on a panel of 250 protein–peptide complexes with experimentally measured affinities and X-ray solved or computationally modeled structures. The complexes were assigned into 22 groups; each group contains a series of cognate peptide ligands that share a common protein receptor. These complexes are available to either their own structures in the PDB database (Berman et al. 2000) or the structures of their cognates where only the peptide ligands are different from but analogous to that in the corresponding complexes. For the latter cases the complex structures were modeled from their cognates using a computational protocol described previously (He et al. 2010).
5. The generated QSAR-improved PPRCP predictor was validated systematically via internal fivefold cross-validation, external blind test and rigorous Monte Carlo cross-validation, and has been successfully used to reproduce protein affinities for 592 human SH3 domain binding peptides and 419 human HLA-A*0201 binding peptides (Han et al. 2013).

## Modeling of MDM2–p53 peptide mutant complex structures

A strategy modified from our recent work (Jin et al. 2013) was used here to construct the complex structure models of MDM2 with p53 peptide mutants. The crystal structure of MDM2 in complex with a wild-type p53 peptide SQETFSDLWKLLPEN (PDB: 4HFZ) (Fig. 1) was used as template to generate the complex structure models of MDM2 with other peptide mutants. The core binding sequence of the wild-type p53 peptide is ETFSDLWKLLPE, which corresponds to the residues 17–28 of p53 protein. The peptide in the complex crystal structure was truncated into the core binding sequence, which was used as template to virtually mutate to other mutants using the SCWRL program (Wang et al. 2008), an automatic tool that predicts optimal rotamer combination for the side chains of the target based on template peptide backbone. The mutated MDM2–peptide complex structure was subjected to a structure minimization procedure with the AMBER03 force field (Duan et al. 2003), where the solvent effect was described using generalized Born (GB) model (Tsui and Case 2000). The maximum number of minimization steps was set to 1,500; the first 500 steps were performed with the steepest descent algorithm, whereas the rest of the steps were carried out with the conjugate gradient algorithm (Hou et al. 2008). The whole procedure of SCWRL mutation and AMBER minimization is illustrated in Fig. 2.

## Molecular dynamics simulation and binding free energy analysis

The modeled MDM2–peptide mutant complex structures were solvated in GB solvent pool and counter ions $Na^+$ were placed on the basis of Coulombic potential to keep the whole system neutral. Atomistic molecular dynamics (MD) simulations were performed to relax and equilibrate the systems, which consisted of a gradual temperature increase from 0 to 300 K over 100 ps, a 1 ns simulation for equilibration, and a following 2 ns simulation for data collection. During the simulations SHAKE algorithm (Ryckaert et al. 1977) was employed to constrain all bonds involving hydrogen atoms, particle mesh Ewald (PME) (Darden et al. 1993) was used to characterize long-range electrostatic interactions, and the time step was set to 2 fs.

The snapshots extracted from the data collection phase were utilized to perform free energy analysis for binding peptide mutants to MDM2, which was fulfilled by molecular mechanics/generalized Born surface area (MM/GBSA) scheme (Kollman et al. 2000). This method considered the total binding free energy ($\Delta G_{total}$) made up of direct non-bonded interaction ($\Delta E_{int}$) and indirect desolvation effect ($\Delta G_{slv}$) (Jing et al. 2013). All computations were carried out with the AMBER03 force field (Duan et al. 2003) supplied in the AMBER9 package (Case et al. 2005).

## Biological assay

Peptides were synthesized by standard $F_{moc}$ solid phase synthesis (Amblard et al. 2006) and fused with a cell-

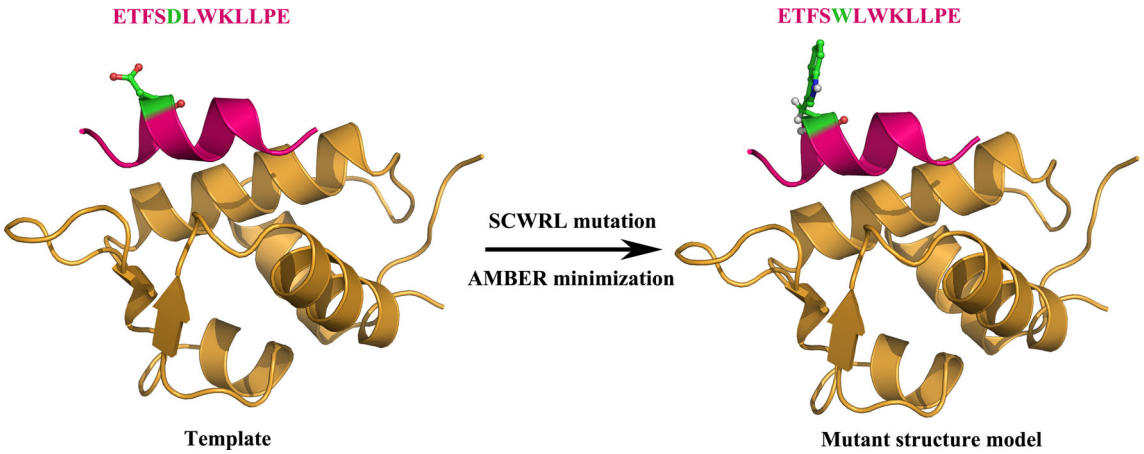


**Fig. 2** Modeling of the complex structure of MDM2 with peptide mutant ETFS**W**LWKLLPE from the template ETFS**D**LWKLLPE

penetrating sequence (Walker et al. 2012). The human breast cancer cell line MCF-7 was obtained from ATCC. The peptides were assayed for their cytotoxic effects on MCF-7 using a protocol modified from a previous report (Cui et al. 2010). Briefly, peptides were dissolved in deionized $H_2O$ and stored at −20 °C. The MCF-7 cells were digested with trypsin into a single-cell suspension and the cell density was adjusted to $2 \times 10^4$/mL. Then, 100 μL cells were cultured in 96 well, which were incubated with the assayed peptide and, for comparison purpose, *cis*-platin for 24 h. Subsequently, 200 μL of MTT and, then, 160 μL of DMSO were added to each well. The effect was determined by a microplate reader.

## Results and discussion

### High-throughput virtual screening of MDM2-binding peptide mutants

The p53 engages a peptide segment ETFSDLWKLLPE in its N-terminal domain to interact with MDM2; the segment is naturally helical and composed of 12 amino acids, corresponding to the sequence region 17–28 of p53 protein. In theory, the 12-residue peptide has totally $19 \times 12 = 228$ single-point mutants and $(19 \times 19) \times (12 \times 11)/2 = 23{,}826$ dual-point mutants, and their complex structures with MDM2 were one-by-one modeled in a high-throughput manner. We have visually surveyed the complex structure models and found most of them are very similar to the crystal structure architecture of MDM2 complexed with wild-type p53 peptide, that is, the peptide mutants adopt helical conformation to tightly interact with the p53-binding site of MDM2. The root-mean-square deviations (rmsd) of backbone atoms of modeled peptide mutants from that of wild-type p53 peptide were calculated by superposing the mutants to the wild type, and their distribution is shown in Fig. 3. As can be seen, the mutations do not influence substantially peptide conformational profile, as all rmsd values are smaller than 0.6 Å and more than half of peptide mutants (62.9 %) have only a miner structural change (rmsd < 0.2 Å) relative to wild-type peptide.

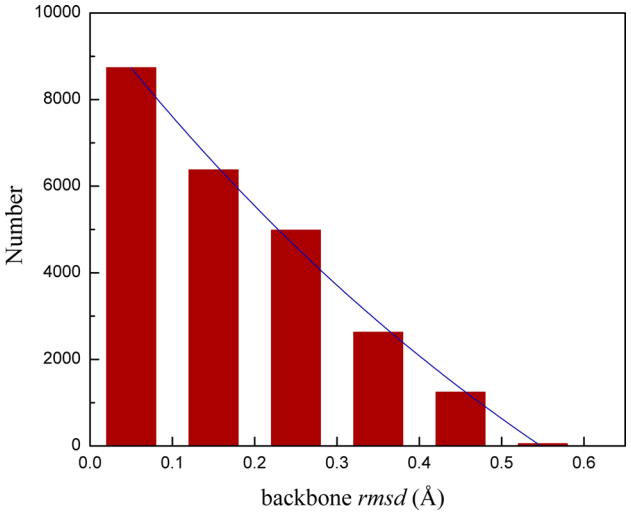


**Fig. 3** The root-mean-square deviation (rmsd) distribution of the backbone atoms of peptide mutants from that of wild-type p53 peptide

Although most of the single- and dual-point mutations can only address a modest influence on peptide binding conformation to MDM2, it is not unexpected that some of which may cast significant effect to MDM2–peptide-binding strength and specificity. In this respect, we employed QSAR-improved PPRCP to efficiently estimate the interaction affinities of the totally 24,054 peptide mutants with MDM2 on the basis of their complex structure models. In a previous study, the QSAR-improved

**(A)**

| p53 peptide and its mutants | Experiment | | Prediction |
|---|---|---|---|
| | $K_d$ (M) | p$K_d$ | p$K_d$ |
| ETFSDLWKLLPE (p53 peptide) | 4.4E-7 | 6.36 | 6.83 |
| ATFSDLWKLLPE | 5.6E -7 | 6.25 | 5.42 |
| EAFSDLWKLLPE | 1.2E -6 | 5.92 | 5.10 |
| ETASDLWKLLPE | nd[a] | nd[a] | 4.97 |
| ETFADLWKLLPE | 2.1E -7 | 6.68 | 6.22 |
| ETFSALWKLLPE | 8.3E -7 | 6.08 | 6.73 |
| ETFSDAWKLLPE | 5.0E-6 | 5.30 | 4.84 |
| ETFSDLAKLLPE | nd[a] | nd[a] | 5.16 |
| ETFSDLWALLPE | 2.3E-7 | 6.64 | 5.67 |
| ETFSDLWKALPE | 7.3E-7 | 6.14 | 6.45 |
| ETFSDLWKLAPE | 2.7E-5 | 4.57 | 5.02 |
| ETFSDLWKLLAE | 5.1E-8 | 7.29 | 6.78 |
| ETFSDLWKLLPA | 2.4E-7 | 6.62 | 6.29 |

[a]nd, the binding affinity of these peptide mutants is too weak to be determined reliably.

**(B)**

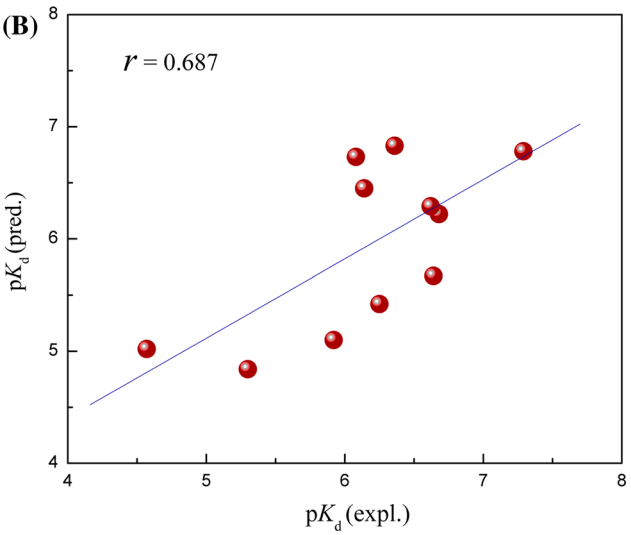


**Fig. 4** **a** A list of experimental and predicted affinities for wild-type p53 peptide and its mutants. **b** The plot of experimental (expl.) against predicted (pred.) affinities for wild-type p53 peptide and its mutants. The experimental affinity values were taken from the report of Li et al. (2010)

PPRCP was demonstrated to be capable of perceiving slight structural change in peptide interactions with SH3 domain and HLA protein (Han et al. 2013), and we therefore hope it can work as well on the MDM2–peptide system. The inference of binding affinity of the numerous peptide mutants to MDM2 was a fast procedure that had been done within several hours, from which the predicted affinities (p$K_d$) for the wild-type p53 peptide and its 12 single-point mutants were compared to experimental values measured by Li et al. (2010) using a Ala-scan mutational analysis. It is seen from Fig. 4 that, given the significant correlation of coefficient of determination $r = 0.687$, the p$K_d$ values predicted using QSAR-improved PPRCP exhibits a good linear correlation with experimental results. In addition, two mutants, ETASDLWKLLPE and ETFSDLAKLLPE, which were determined in vitro as weak MDM2 binders, were properly predicted to have relatively low affinities (p$K_d$ = 4.97 and 5.16, respectively) for MDM2.

The histogram distribution of predicted affinity differences ($\Delta pK_d = pK_d^{mt} - pK_d^{wt}$) of 24054 peptide mutants (*mt*) to the wild-type p53 peptide (*wt*) is shown in Fig. 5, which gives a straightforward insight into the change in p53 peptide affinity upon residue mutations. It is evident that most mutations (93.3 %) would impair the binding capability of p53 peptide to MDM2, indicating that the sequence pattern of wild-type peptide has been evolutionarily optimized to match well its cognate MDM2 receptor, and most of slight changes in the pattern would undermine the well-defined interactions between the peptide and MDM2. However, there were also a few number of mutants (6.7 %) that exhibited improved affinities relative to p53

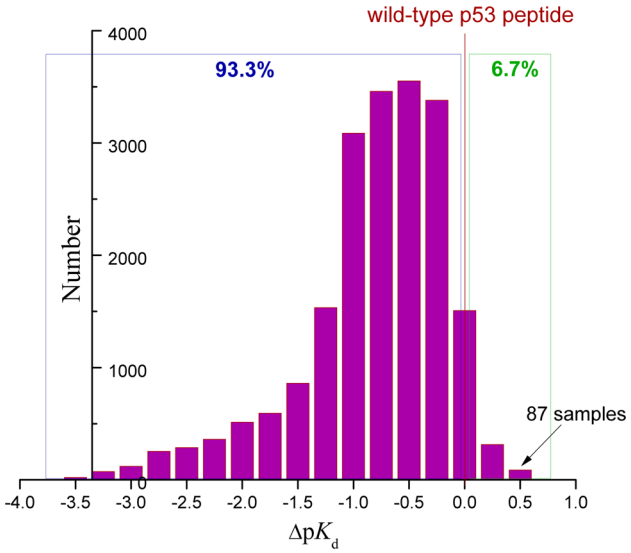


**Fig. 5** Histogram distribution of the differences in binding affinity ($\Delta pK_d$) of 24,054 peptide mutants to the wild-type p53 peptide

peptide, although the improved values are relatively moderate ($\Delta pK_d < 1$). A total of 1,612 mutants, including 13 single-point mutants and 1,599 dual-point mutants, were predicted to possess higher affinity than the wild-type p53 peptide. Because of calculation error and systematic bias, the minor improvements in predicted affinity could be regarded as noise and thus were not considered in this study. Here, only the peptide mutants located within the maximal bin of $\Delta pK_d = 0.5$ (i.e., $\Delta pK_d > 0.375$) were further examined to exploit more potent MDM2 binders, which include 87 samples.

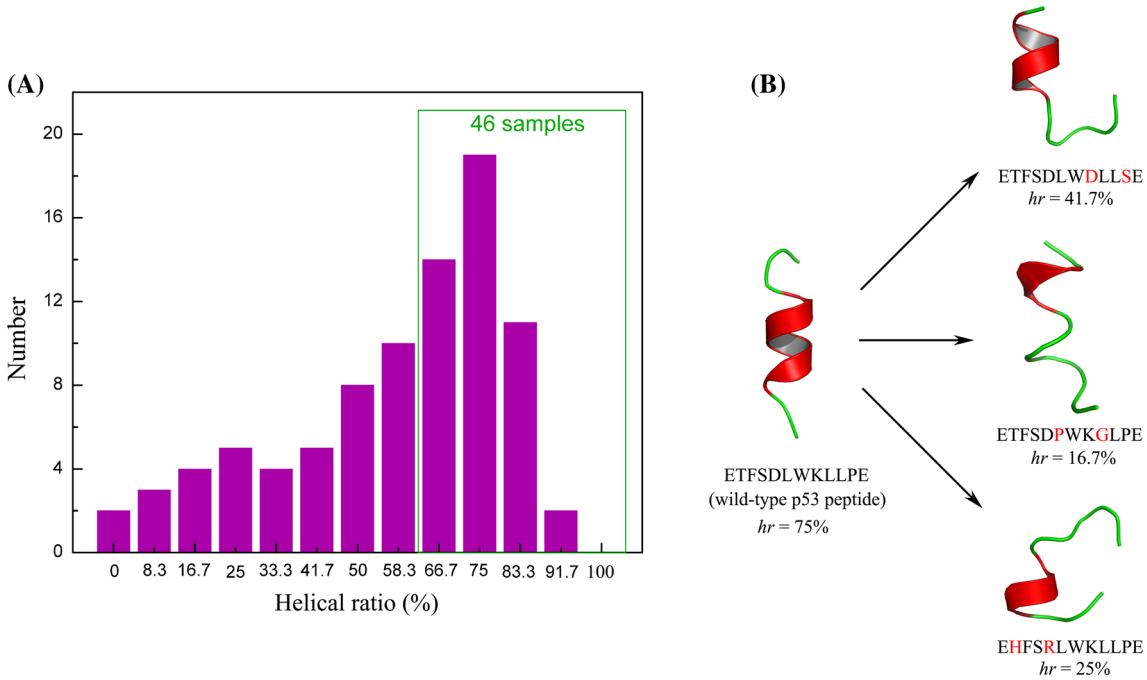


**Fig. 6** **a** The distribution of predicted helical ratios for the 87 predicted high-affinity peptide mutants. **b** Some examples of peptide mutants with low helical ratio (hr)

According to previous survey of various protein–peptide complex crystal structures deposited in the PDB database (Berman et al. 2000), it was suggested that high-activity peptides are more likely to be pre-organized into helical configuration in unbound state, thus minimizing the entropic cost of binding to their protein receptors (London et al. 2010). In fact, most existing active peptides with capability of targeting protein–protein interactions are naturally helical (Jochim and Arora 2009) and, very recently, a designed peptide drug possessing enhanced therapeutic potency against the p53–MDM2 system was structurally constrained into α-helix using hydrocarbon stapling (Chang et al. 2013). Therefore, we herein employed the PEP-FOLD server (Thévenet et al. 2012) to model spatial structures for the 87 predicted high-affinity mutants as well as wild-type p53 peptide in their free state. The wild-type peptide was predicted to have a good pre-organized advanced structure, with helical ratio (hr) of 75 % (9/12 × 100 %). The distribution of predicted helical ratios for the 87 mutants is shown in Fig. 6a, from which it is seen that most mutations do not influence substantially the advanced structure of p53 peptide, but there were few mutants such as ETFSDLWDLLSE (hr = 41.7 %), ETFSDPWKGLPE (hr = 16.7 %) and EHFSRLWKLLPE (hr = 25 %) that would significantly undermine the helical configuration (Fig. 6b). In this respect, we excluded those with hr <66.7 % (8/12 × 100 %) and, as a result, 46 peptide mutants with satisfactory pre-organized helical structures were selected for subsequent analysis.

## MD simulation, MM/GBSA analysis and biological assay

To quantify the binding strength of p53 peptide and its 46 mutants to MDM2, we employed the post-MM/GBSA technique to empirically estimate their interaction potencies. The MM/GBSA analysis was performed over various snapshots extracted evenly from the last 2 ns MD equilibrium. In this way, the total binding energy $\Delta G_{\text{total}}$ of a peptide to MDM2 can be decomposed into direct non-bonded potential $\Delta E_{\text{int}}$ between the MDM2 and peptide, and the indirect desolvation energy $\Delta G_{\text{slv}}$ due to solvent effect. According to the calculations, the nonbonded interactions form intensive networks at complex interfaces that contribute considerably to the total binding energy. This favorable energetic contribution, however, would be compensated partially by the unfavorable effect arising from desolvation penalty due to the binding, resulting in a wide spectrum of the MDM2–peptide binding free energies ($\Delta G_{\text{total}}$ ranges from $\sim -80$ to $-160$ kcal/mol).

Eight peptide mutants with significant binding energy ($\Delta G_{\text{total}} < -120$ kcal/mol), high affinity ($pK_d > 7.4$) and large helical ratio (hr > 60 %) were considered as highly promising candidates, which were synthesized, purified and assayed to determine their cytotoxicity on breast cancer cell line MCF-7, and the resulting $IC_{50}$ values as well as other relevant information are provided in Table 1. Satisfactorily, six of these assayed peptides (ETFSDWWKLLVE, ESFSDLWKLLAE, ETFADYWKLLPE, ETFVDLWKLLAE,

**Table 1** A list of eight putative high-activity peptide mutants, three modified peptide mutants as well as the wild-type p53 peptide and *cis*-platin for comparison

| Peptide | | Prediction | | Calculation (kcal/mol) | | | Experiment |
|---|---|---|---|---|---|---|---|
| Name | Sequence[a] | p$K_d$ | hr (%) | $\Delta E_{int}$ | $\Delta G_{slv}$ | $\Delta G_{total}$ | $IC_{50}$ (μM) |
| *cis*-Platin | – | – | – | – | – | – | 4.3 |
| *wt* | $^{17}$ETFSDLWKLLPE$^{28}$ | 6.83 | 75 | −168.3 | 64.2 | −104.1 | 182.6 |
| *mt*_L22 W/P27 V | ETFSDWWKLLVE | 7.74 | 75 | −173.7 | 49.0 | −124.7 | 69.4 |
| *mt*_K24 N/P27T | ETFSDLWNLLTE | 7.58 | 66.7 | −189.2 | 52.9 | −136.3 | Inactive |
| *mt*_T18S/P27A | ESFSDLWKLLAE | 7.62 | 83.9 | −170.0 | 30.8 | −159.2 | 58.9 |
| *mt*_S20A/L22Y | ETFADYWKLLPE | 7.76 | 66.7 | −170.9 | 30.7 | −140.2 | 21.6 |
| *mt*_D21E/L26I | ETFSELWKLIPE | 7.57 | 75 | −187.7 | 41.0 | −146.7 | Inactive |
| *mt*_S20 V/P27A | ETFVDLWKLLAE | 7.79 | 83.9 | −177.9 | 39.4 | −138.5 | 34.4 |
| *mt*_E17L/L22F | LTFSDFWKLLPE | 7.52 | 75 | −178.6 | 52.5 | −126.1 | 137.0 |
| *mt*_L22 W/P27A | ETFSDWWKLLAE | 7.70 | 75 | −191.2 | 43.2 | −148.0 | 16.3 |
| *mt*_E17L/L22 W/P27A | LTFSDWWKLLAE | 7.76 | 75 | −196.4 | 43.9 | −152.5 | 15.1 |
| *mt*_T18S/L22 W/P27A | ESFSDWWKLLAE | 7.72 | 66.7 | −194.5 | 47.3 | −147.2 | 27.0 |
| *mt*_S20A/L22 W/P27A | ETFADWWKLLAE | 7.74 | 75 | −196.5 | 28.2 | −168.3 | 8.7 |

[a] The mutated residues are colored in red

LTFSDFWKLLPE and ETFSDWWKLLAE) were measured to possess suppressing potency against MCF-7, albeit other two mutants (ETFSDLWNLLTE and ETFSELWKLIPE) have no observable activity in the biological assay. It is known that the cytotoxicity is not only determined by the direct interaction between MDM2 and peptide, but also contributed from some other factors such cell permeation and metabolism. Therefore, the two inactive peptides might be good binders of MDM2 but bad attackers of breast cancer cells. The $IC_{50}$ values of six potent peptides range from 16.3 to 137.0 μM, which are better than that of wild-type p53 peptide ($IC_{50}$ = 182.6 μM) and close to that of classical anticancer agent *cis*-platin ($IC_{50}$ = 4.3 μM).

Further, we have investigated the linear correlations of experimentally measured activity (p$IC_{50}$) with theoretically derived affinity (p$K_d$), helical ratio (hr) and binding free energy ($\Delta G_{total}$) for p53 peptide and its six active mutants. As shown in Fig. 7, the p$K_d$, hr and $\Delta G_{total}$ exhibit moderate, low and high correlations with p$IC_{50}$ (their Pearson coefficients $R_p$ are 0.684, −0.187 and −0.776, respectively), indicating that the $\Delta G_{total}$ could be used as a good predictor for peptide activity. When we performed multiple linear regression for p$IC_{50}$ with p$K_d$, hr and $\Delta G_{total}$, a more significant correlation was obtained (Eq. 1), although the good fitting ability does not mean a strong predictive power if considering that only limited samples were used to derive the regression.

$$\mathrm{pIC}_{50} = 3.14 + 0.49 \times \mathrm{p}K_d - 5.5 \times \mathrm{hr} - 0.12 \times \Delta G_{\mathrm{total}} \quad (r = 0.805, F = 5.14, p = 0.106) \tag{1}$$

## Structure-based modification of peptides

The mutant ETFSDWWKLLAE (*mt*_L22 W/P27A) showed significant cytotoxic effect on MCF-7 ($IC_{50}$ = 16.3 μM). Based on its sequence pattern, this peptide was modified separately with mutations E17L, T18S and S20A—these three mutations were found to be capable of improving the biological activity of p53 peptide, as shown in Table 1. As a result, three new triple-point mutants LTFSDWWKLLAE (*mt*_E17L/L22 W/P27A), ESFSDWWKLLAE (*mt*_T18S/L22 W/P27A) and ETFADWWKLLAE (*mt*_S20A/L22 W/P27A) were obtained, and their affinities p$K_d$, helical ratios hr and binding free energies $\Delta G_{total}$ to MDM2 were calculated to list in Table 1. As can be seen, the p$K_d$ and $\Delta G_{total}$ of the three modified mutants exhibit a moderate or considerable improvement as compared to the parent peptide *mt*_L22 W/P27A, although hr has no substantial change for these mutants. Further, we performed in vitro assay to determine biological activities for the mutants, resulting in $IC_{50}$ values of 15.1, 27.0 and 8.7 μM, respectively. As might be expected, the activity changes are not very significant upon the mutations; the $IC_{50}$ values of mutants *mt*_E17L/L22 W/P27A and *mt*_S20A/L22 W/P27A are improved modestly and moderately, respectively, relative to that of parent *mt*_L22 W/P27A, whereas the *mt*_T18S/L22 W/P27A displays lower biological activity than the parent.

By visually examining the nonbonded interactions across the complex interface of different peptide mutants as well as wild-type p53 peptide with MDM2 (Fig. 8), it is found that the L22 W/P27A dual mutation could introduce a number of van der Waals contacts and hydrophobic interactions into the complex system and, in particular, the aromatic ring of the mutated W22 residue can form a

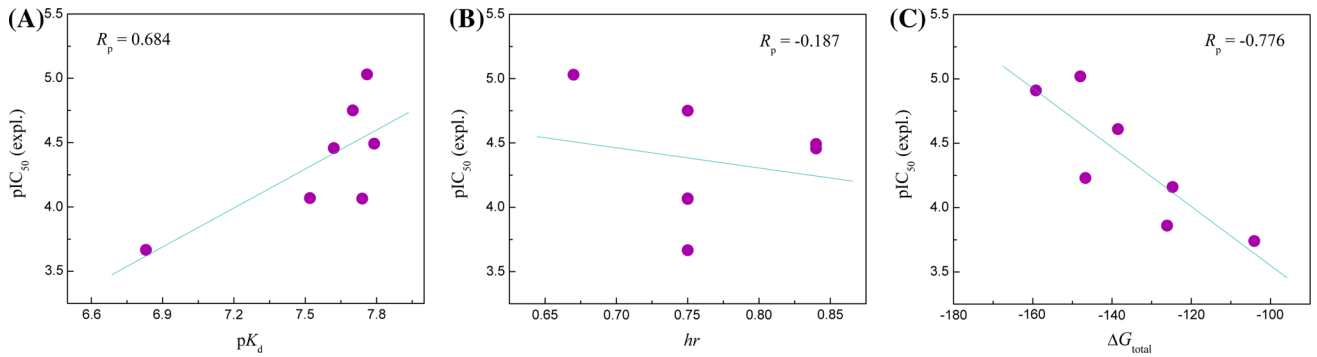


**Fig. 7** The plots of experimentally measured activity ($pIC_{50}$) against theoretically determined affinity ($pK_d$) (**a**), helical ratio (hr) (**b**) and binding free energy ($\Delta G_{total}$) (**c**) for p53 peptide and its six active mutants

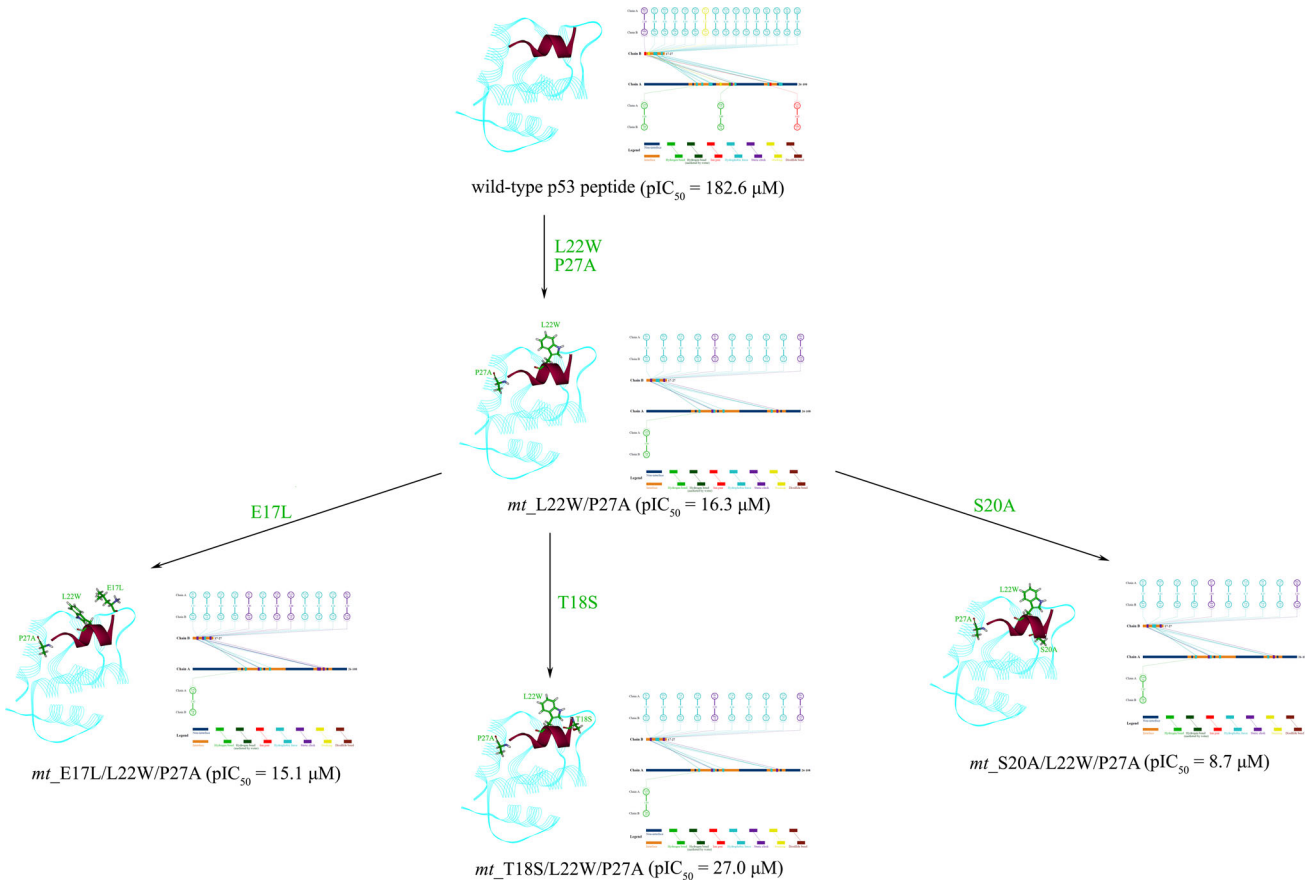


**Fig. 8** Schematic representation of the mutation procedure of wild-type p53 peptide to dual-point mutant *mt*_L22 W/P27A and, further, to triple-point mutants *mt*_E17L/L22 W/P27A, *mt*_T18S/L22 W/P27A and *mt*_S20A/L22 W/P27A. The nonbonded interactions across the complex interface of MDM2 with p53 peptide and its mutants were generated using the 2D-GraLab program (Zhou et al. 2009) based on MD equilibrated complex structure models

geometrically satisfactory cation–π interaction with Lys94 residue of MDM2. These observed additional nonbonded effects are used to explain the significant enhancement in peptide activity due to the mutation of wild-type p53 peptide to the mutant *mt*_L22 W/P27A ($IC_{50}$ value decreases from 182.6 to 16.3 μM). A further mutation E17L, T18S or S20A would alter slightly the local structural arrangements and nonbonded profiles of complex interface, leading to a moderate change in peptide activity ($IC_{50}$ value changes from 16.3 to 15.1, 27.0 or 8.7 μM). The E17L mutation could enhance hydrophobic potential for MDM2–peptide system, but this mutation is located at

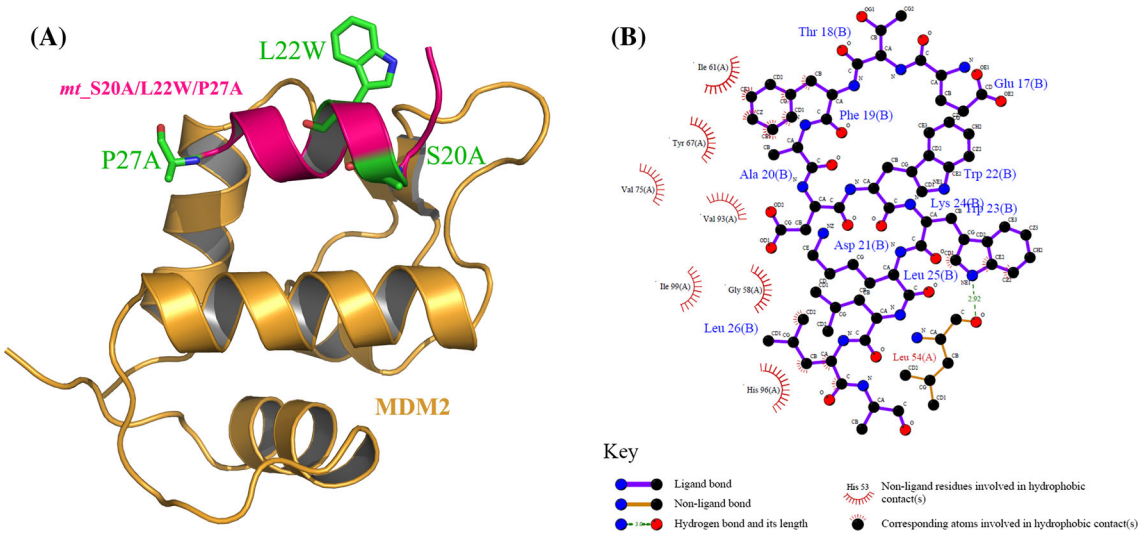


**Fig. 9** **a** Stereoview of the complex structure architecture of MDM2 with the high-activity mutant *mt*_S20A/L22 W/P27A. **b** Schematic representation of the nonbonded interactions across the complex interface. This plot was generated using the LigPlot program (Wallace et al. 1995)

the N-terminus of peptide and thus can only confer a quite modest effect for the complex ($IC_{50}$ value improves from 16.3 to 15.1 μM); the T18S mutation does not have any observable influence on the nonbonded profile of complex, but associated activity shows a minor reduction upon the mutation ($IC_{50}$ value increases from 16.3 to 27.0 μM); the S20A mutation results in a perceivable increase in peptide activity ($IC_{50}$ value changes from 16.3 to 8.7 μM), which improves the packing density of nonpolar contacts at the complex interface and defines a number of weak chemical forces such as hydrophobic interactions with the residues Trp67, Val75 and Val93 of MDM2 (Fig. 9).

## Conclusions

In the current study, we have proposed a synthetic pipeline to design novel p53-derived peptides with high potency to target the p53–MDM2 interaction that promotes tumor development and progression. In the procedure, a knowledge-based statistical potential that was derived from protein–peptide interface clusters and improved by protein–peptide complexes with experimentally measured affinities was applied to high-throughput virtual screening of all single- and dual-point mutants of p53 peptide. As a result, 46 peptide mutants with both high predicted affinity and large helical ratio were examined in detail using atomistic MD simulations and post-MM/GBSA analysis, from which a number of highly promising mutants were selected to perform biological assay to determine their cytotoxicity on human breast cancer cells. As might be expected, most of the assayed mutants exhibited moderate or high biological activity, some of which showed cytotoxic effects even close to that of classical anticancer agent *cis*-platin. Further, we have modified the most active peptide, a dual-point mutant, with three potential single-point mutations, separately resulting in three triple-point mutants. Biological analysis demonstrated that one of the three mutants received substantially enhanced activity due to the mutation, which can be explained well at molecular level by analyzing nonbonded interactions across the complex interface of MDM2–peptide system.

**Acknowledgments** This work was supported by the National Natural Science Foundation of China (Grant No. 81372829).

**Conflict of interest** The authors declare that they have no conflict of interest.

## References

Amblard M, Fehrentz JA, Martinez J, Subra G (2006) Methods and protocols of modern solid phase peptide synthesis. Mol Biotech 33:239–254

Anil B, Riedinger C, Endicott JA, Noble ME (2013) The structure of an MDM2–Nutlin-3a complex solved by the use of a validated MDM2 surface-entropy reduction mutant. Acta Crystallogr D 69:1358–1366

Berman HM, Westbrook J, Feng Z, Gilliland G, Bhat TN, Weissig H, Shindyalov IN, Bourne PE (2000) The protein data bank. Nucleic Acids Res 28:235–242

Bray F, McCarron P, Parkin DM (2004) The changing global patterns of female breast cancer incidence and mortality. Breast Cancer Res 6:229–239

Caffarel MM, Andradas C, Pérez-Gómez E, Guzmán M, Sánchez C (2012) Cannabinoids: a new hope for breast cancer therapy? Cancer Treat Rev 38:911–918

Case DA, Cheatham TE, Darden T, Gohlke H, Luo R, Merz KM (2005) The Amber biomolecular simulation programs. J Comput Chem 26:1668–1688

Chang YS, Graves B, Guerlavais V, Tovar C, Packman K, To KH, Olson KA, Kesavan K, Gangurde P, Mukherjee A, Baker T, Darlak K, Elkin C, Filipovic Z, Qureshi FZ, Cai H, Berry P, Feyfant E, Shi XE, Horstick J, Annis DA, Manning AM, Fotouhi N, Nash H, Vassilev LT, Sawyer TK (2013) Stapled α-helical peptide drug development: a potent dual inhibitor of MDM2 and MDMX for p53-dependent cancer therapy. Proc Natl Acad Sci USA 110:3445–3454

Chene P (2004) Inhibition of the p53–MDM2 interaction: targeting a protein–protein interface. Mol Cancer Res 2:20–28

Chi SW, Lee SH, Kim DH, Ahn MJ, Kim JS, Woo JY, Torizawa T, Kainosho M, Han KH (2005) Structural details on mdm2–p53 interaction. J Biol Chem 280:38795–38802

Coles C, Condie A, Chetty U, Steel CM, Evans HJ, Prosser J (1992) p53 mutations in breast cancer. Cancer Res 52:5291–5298

Cui W, Wei Z, Chen Q, Cheng Y, Geng L, Zhang J, Chen J, Hou T, Ji M (2010) Structure-based design of peptides against G3BP with cytotoxicity on tumor cells. J Chem Inf Model 50:380–387

Darden T, York D, Pedersen L (1993) Particale mesh Ewald and *N*.log(*N*) method for Ewald sums in large systems. J Chem Phys 98:10089–10092

Duan Y, Wu C, Chowdhury S, Lee MC, Xiong GM, Zhang W (2003) A point-charge force field for molecular mechanics simulations of proteins based on condensed-phase quantum mechanical calculations. J Comput Chem 24:1999–2012

Gasco M, Shami S, Crook T (2002) The p53 pathway in breast cancer. Breast Cancer Res 4:70–76

Han K, Wu G, Lv F (2013) Development of QSAR-improved statistical potential for the structure-based analysis of protein–peptide binding affinities. Mol Inf 32:783–792

He P, Wu W, Wang HD, Yang K, Liao KL, Zhang W (2010) Toward quantitative characterization of the binding profile between the human amphiphysin-1 SH3 domain and its peptide ligands. Amino Acids 38:1209–1218

Hou T, Zhang W, Case DA, Wang W (2008) Characterization of domain–peptide interaction interface: a case study on the amphiphysin-1 SH3 domain. J Mol Biol 376:1201–1214

Hu B, Gilkes DM, Chen J (2007) Efficient p53 activation and apoptosis by simultaneous disruption of binding to MDM2 and MDMX. Cancer Res 67:8810–8817

Jemal A, Bray F, Center MM, Ferlay J, Ward E, Forman D (2011) Global cancer statistics. CA Cancer J Clin 61:69–90

Jin R, Ma Y, Qin L, Ni Z (2013) Structure-based prediction of domain–peptide binding affinity by dissecting residue interaction profile at complex interface: a case study on CAL PDZ domain. Protein Pept Lett 20:1018–1028

Jing T, Feng J, Li D, Liu J, He G (2013) Rational design of angiotensin-I-converting enzyme inhibitory peptides by integrating in silico modeling and an in vitro assay. ChemMedChem 8:1057–1066

Jochim AL, Arora PS (2009) Assessment of helical interfaces in protein–protein interactions. Mol BioSyst 5:924–926

Kollman PA, Massova I, Reyes C, Kuhn B, Huo SH (2000) Calculating structures and free energies of complex molecules: combining molecular mechanics and continuum models. Acc Chem Res 33:889–897

Li C, Pazgier M, Li C, Yuan W, Liu M, Wei G, Lu WY, Lu W (2010) Systematic mutational analysis of peptide inhibition of the p53–MDM2/MDMX interactions. J Mol Biol 398:200–213

London N, Movshovitz-Attias D, Schueler-Furman O (2010) The structural basis of peptide–protein binding strategies. Structure 18:188–199

Mitchell JBO, Laskowski RA, Alex A, Thornton JM (1999) Potential of mean force describing protein–ligand interactions: I. Generating potential. J Comput Chem 20:1165–1176

Petsalaki E, Russell RB (2008) Peptide-mediated interactions in biological systems: new discoveries and applications. Curr Opin Biotech 19:344–350

Popowicz GM, Domling A, Holak TA (2011) The structure-based design of Mdm2/Mdmx–p53 inhibitors gets serious. Angew Chem Int Ed 50:2680–2688

Ryckaert J, Ciccotti G, Berendsen HJC (1977) Numerical-integration of cartesian equations of motion of a system with constraints: moleculardynamics of *n*-alkanes. J Comput Phys 23:327–341

Thévenet P, Shen Y, Maupetit J, Guyon F, Derreumaux P, Tufféry P (2012) PEP-FOLD: an updated de novo structure prediction server for both linear and disulfide bonded cyclic peptides. Nucleic Acids Res 40:W288–W293

Tsui V, Case DA (2000) Theory and applications of the generalized Born solvation model in macromolecular simulations. Biopolymers 56:275–291

Vanhee P, Reumers J, Stricher F, Baeten L, Serrano L, Schymkowitz J, Rousseau F (2010) PepX: a structural database of non-redundant protein–peptide complexes. Nucleic Acids Res 38:D545–D551

Walker L, Perkins E, Kratz F, Raucher D (2012) Cell penetrating peptides fused to a thermally targeted biopolymer drug carrier improve the delivery and antitumor efficacy of an acid-sensitive doxorubicin derivative. Int J Pharm 436:825–832

Wallace AC, Laskowski RA, Thornton JM (1995) LIGPLOT: a program to generate schematic diagrams of protein–ligand interactions. Protein Eng 8:127–134

Wang Q, Canutescu AA, Dunbrack RL (2008) SCWRL and MolIDE: computer programs for side-chain conformation prediction and homology modeling. Nat Protoc 3:1832–1847

Wang S, Zhao Y, Bernard D, Aguilar A, Kumar S (2012) Targeting the MDM2–p53 protein–protein interaction for new cancer therapeutics. Top Med Chem 8:57–80

Yang P, Du CW, Kwan M, Liang SX, Zhang GJ (2013) The impact of p53 in predicting clinical outcome of breast cancer patients with visceral metastasis. Sci Rep 3:2246

Zhou P, Tian F, Shang Z (2009) 2D depiction of nonbonding interactions for protein complexes. J Comput Chem 30:940–951

Zhou P, Tian F, Ren Y, Shang Z (2010) Systematic classification and analysis of themes in protein–DNA recognition. J Chem Inf Model 50:1476–1488

Zhou P, Wang C, Ren Y, Yang C, Tian F (2013) Computational peptidology: a new and promising approach to therapeutic peptide design. Curr Med Chem 20:1985–1996